Structural signatures of water-soluble organic aerosols in contrasting environments in South America and Western Europe[☆]

Regina M.B.O. Duarte [a, *], João T.V. Matos [a], Andreia S. Paula [a], Sónia P. Lopes [a],
Guilherme Pereira [b], Pérola Vasconcellos [b], Adriana Gioda [c], Renato Carreira [c],
Artur M.S. Silva [d], Armando C. Duarte [a], Patricia Smichowski [e], Nestor Rojas [f],
Odon Sanchez-Ccoyllo [g]

[a] Department of Chemistry & CESAM, University of Aveiro, 3810-193, Aveiro, Portugal
[b] Institute of Chemistry, University of São Paulo, São Paulo, Brazil
[c] Department of Chemistry, Pontifical Catholic University of Rio de Janeiro, Rio de Janeiro, Brazil
[d] Department of Chemistry & QOPNA, University of Aveiro, 3810-193, Aveiro, Portugal
[e] Comisión Nacional de Energía Atómica, Buenos Aires, Argentina
[f] National University of Colombia, Bogotá, Colombia
[g] National Meteorology and Hydrology Service of Peru, Lima, Peru

ARTICLE INFO

ABSTRACT

This study describes and compares the key structural units present in water-soluble organic carbon (WSOC) fraction of atmospheric aerosols collected in different South American (Colombia – Medellín and Bogotá, Peru – Lima, Argentina – Buenos Aires, and Brazil – Rio de Janeiro, São Paulo, and Porto Velho, during moderate (MBB) and intense (IBB) biomass burning) and Western European (Portugal – Aveiro and Lisbon) locations. Proton nuclear magnetic resonance (^{1}H NMR) spectroscopy was employed to assess the relative distribution of non-exchangeable proton functional groups in aerosol WSOC of diverse origin, for the first time to the authors' knowledge in South America. The relative contribution of the proton functional groups was in the order H-C > H−C−C= > H-C-O > Ar-H, except in Porto Velho during MBB, Medellín, Bogotá, and Buenos Aires, for which the relative contribution of H-C-O was higher than that of H-C-C=. The ^{1}H NMR source attribution confirmed differences in aging processes or regional sources between the two geographic regions, allowing the differentiation between urban combustion-related aerosol and biological particles. The aerosol WSOC in Aveiro, Lisbon, and Rio de Janeiro during summer are more oxidized than those from the remaining locations, indicating the predominance of secondary organic aerosols. Fresh emissions, namely of smoke particles, becomes important during winter in Aveiro and São Paulo, and in Porto Velho during IBB. The biosphere is an important source altering the chemical composition of aerosol WSOC in South America locations. The source attribution in Medellín, Bogotá, Buenos Aires, and Lima confirmed the mixed contributions of biological material, secondary formation, as well as urban and biomass burning emissions. Overall, the information and knowledge acquired in this study provide important diagnostic tools for future studies aiming at understanding the water-soluble organic aerosol problem, their sources and impact at a wider geographic scale.

© 2017 Elsevier Ltd. All rights reserved.

1. Introduction

Nowadays, it is firmly established that atmospheric organic aerosols (OA) are inexorably linked to both climate change and adverse health outcomes (e.g., Kanakidou et al., 2005; Heal et al., 2012; Booth et al., 2012; Laskin et al., 2015). OA have been shown to be ubiquitous in urban, rural, and remote locations, representing an important component of air particulate matter (PM) (Jimenez et al., 2009; references therein; Putaud et al., 2010). The OA are highly dynamic, with a myriad of sources and formation

---

mechanisms contributing significantly to the OA burden in the atmosphere. OA can be directly emitted into the atmosphere (from both natural and anthropogenic sources) or formed *in situ* from chemical reactions (i.e., secondary formation). Once in the atmosphere, OA can also undergo a wide variety of oxidation processes that modify their physico-chemical properties (Hallquist et al., 2009). One of the most important attributes of atmospheric OA for both climate and health impacts is their chemical composition. It has been shown that most OA mass at urban and anthropogenically influenced rural/remote areas is dominated by oxygenated species (e.g., Zhang et al., 2007; Duarte et al., 2007, 2015; Crilley et al., 2014; Lopes et al., 2015), and it contains both water-soluble and water-insoluble organic components. The water-soluble organic carbon (WSOC) fraction is usually below 70% of the organic carbon (OC) present in the air particulate matter (e.g., Duarte et al., 2007; Wozniak et al., 2012; Zhang et al., 2014; Lopes et al., 2015). The enrichment of air particles in WSOC and its mixing state with the inorganic counterpart plays an important role in several atmospheric processes. The WSOC might potentially affect the properties that determine the aerosols' ability to act as cloud condensation nuclei (Dinar et al., 2006; Padró et al., 2010). It has been also suggested that the WSOC might contribute to the absorption of solar radiation, and thus atmospheric heating and global climate change (Dinar et al., 2008; Mladenov et al., 2010). Furthermore, the wet deposition fluxes of atmospheric water-soluble organic matter (WSOM) indicate that it may be an important temporal source of OC to surface waters and, thus, playing an important role in the global carbon cycle (Jurado et al., 2008). From the public health perspective, there are evidences on the association between aerosol OC and adverse health effects (Cassee et al., 2013), with the secondary OC component (more water-soluble) being suggested as a valuable air quality metric. Despite its significance, the multitude of molecular forms, sources, and atmospheric reactivity makes a complete characterization of aerosol WSOC extremely difficult. Nevertheless, determining its structural composition is needed to explore its dynamics as well as its sources and formation mechanisms. Furthermore, targeting the chemical composition of aerosol WSOC is also essential for climatic and epidemiological studies, whose results are critical to support and evaluate informed policies on atmospheric pollution reduction at regional and global levels (Cassee et al., 2013; Saffari et al., 2014; Atkinson et al., 2015).

In the quest for untangle the complex molecular composition of the water-soluble component of OA, it has been shown that the WSOC consists of a highly diverse suite of oxygenated compounds, including dicarboxylic acids, keto-carboxylic acids, aliphatic aldehydes and alcohols, saccharides, saccharide anhydrides, aromatic acids, phenols, but also amines, amino acids, organic nitrates, and organic sulfates (e.g., Duarte et al., 2007, 2008, 2015; Timonen et al., 2013; Ng et al., 2010; Cleveland et al., 2012; Shakya et al., 2012; Pietrogrande et al., 2013; Chalbot et al., 2014; Paglione et al., 2014; Lopes et al., 2015; Chalbot et al., 2016). A common ground of the available compositional datasets on aerosol WSOC is that they refer to studies carried out in urban, rural, and remote locations predominantly at North America and Europe, besides a few urban sites in Asia. On the other hand, comprehensive structural identification within the complex aerosol WSOC mixture has been rarely reported for Southern Hemisphere locations. Most field studies within this region have included measurements of ambient concentrations of OC, elemental carbon (EC), and WSOC, specific organic markers (e.g., *n*-alkanes, PAHs, and levoglucosan), or the amount of hydrocarbon-like and oxygenated OA components [e.g., in Brisbane (Australia), Tanzania (rural background site), São Paulo (Brazil), Rondônia (Amazon Basin, Brazil), Buenos Aires (Argentina), Bogotá (Colombia), and Santiago (Chile)] (Graham et al., 2002;

Mayol-Bracero et al., 2002; Tagliavini et al., 2006; Vasconcellos et al., 2010, 2011; Mkoma and Kawamura, 2013; Crilley et al., 2014; Souza et al., 2014; De Oliveira Alves et al., 2015; Villalobos et al., 2015). Although these studies have provided a glimpse into the bulk chemical makeup of OA, the current understanding of the role of aerosol WSOC in global climate change still is incomplete. In order to draw a meaningful picture of the climate and health-related properties of atmospheric WSOC, one first needs to understand its chemical composition at a wider geographic scale. It becomes, therefore, crucial to lengthen the observational records by improving the current knowledge on the structural composition of aerosol WSOC and, simultaneously, glean additional information on how these compositional features change across different environments and ambient conditions.

The objective of this study was to investigate and compare the structural characteristics of WSOC in atmospheric aerosols collected in different locations (urban, suburban, and forest) at South America (Colombia – Medellín and Bogotá, Peru – Lima, Argentina – Buenos Aires, and Brazil – Rio de Janeiro, São Paulo and Porto Velho) and Western Europe (Portugal – Aveiro and Lisbon). The approach chosen to fulfill this objective encompasses functional group analysis using proton nuclear magnetic resonance (^{1}H NMR) spectroscopy. This strategy has been successfully applied to different aerosol WSOC samples, namely from biomass burning aerosols, marine organic aerosols, secondary organic aerosols (SOA), urban aerosols, rural aerosols, and size-fractionated atmospheric aerosols (Graham et al., 2002; Tagliavini et al., 2006; Decesari et al., 2007; Chalbot et al., 2014, 2016; Lopes et al., 2015). In this study, the acquired ^{1}H NMR datasets were further used to build fingerprints for source contribution analysis, following the method of Decesari et al. (2007). With this study it is expected to get a deeper insight into the yet unsolved structural composition of aerosol WSOC at different Southern Hemisphere locations, and to understand possible composition variations in WSOC due changes in their sources at contrasting environments.

2. Materials and methods

2.1. Aerosol samples collection

Aerosol samples were collected at nine different locations, extending from Aveiro and Lisbon (Portugal) located at the West European Coast, to Medellín and Bogotá (Colombia), Lima (Peru), Porto Velho, Rio de Janeiro and São Paulo (Brazil), and Buenos Aires (Argentina), located in South America (Fig. 1). Table 1 summarizes relevant information about the studied locations, including the particle size, sampling period, season, sampling duration, and air mass transport features during the aerosol sampling campaigns. The meteorological data, including air temperature, accumulated rainfall, relative humidity, solar radiation, maximum wind velocity, and air masses origin, across the different field campaigns are available in Table S1, in Supporting Information (SI).

In Aveiro, with approximately 60,000 inhabitants, the aerosol sampling occurred at the Campus (Santiago) of the University of Aveiro, on a rooftop approximately 20 m above the ground. The sampling site is located on the west coast of Portugal, 10 km from the Atlantic Ocean, and very close to the city center. An industrial complex, which includes the production of nitric acid, aniline, nitrobenzene and chlorinate compounds, is located 10 km to the North of Aveiro. A total of eight high-volume PM$_{2.5}$ (particulate matter with aerodynamic diameter < 2.5 μm) samples were collected on quartz fibre filters (20.3 × 25.4 cm; Whatman QM-A, GE Healthcare Life Sciences), on a weekly basis (7 days in continuum), during July–August 2010 [*n* = 3, Summer (SU)] and December 2010–February 2011 [*n* = 5, Winter (WI)] in order to

Fig. 1. Location of the nine aerosol sampling sites in South America and Western Europe.

Table 1
Summary of atmospheric aerosol sampling conditions at each studied location (additional details are available in Table S1 and section S1, in Supporting Information).

Location	Particle Size	Sampling Period	Sampling Duration	Season	Origin of Air Masses [c]	Reference
Medellín (Colombia)	PM$_{10}$	June 2010 (*n* = 12) [a]	24 h	Dry	Continent	This study
Bogotá (Colombia)	PM$_{10}$	Nov—Dec 2008 (*n* = 12)	24 h	Wet	Continent	Vasconcellos et al. (2011)
Lima (Peru)	PM$_{10}$	June—Aug 2010 (*n* = 10)	24 h	Winter	Marine/Continent	This study
Buenos Aires (Argentina)	PM$_{10}$	Aug—Sept 2008 (*n* = 13)	24 h	Winter/Spring	Marine/Continent	Vasconcellos et al. (2011)
Porto Velho (PV, Brazil)	PM$_{10}$	Aug—Oct 2011 (*n* = 17) — IBB [b]	47—168 h	Winter/Spring	Marine/Continent	De Oliveira Alves et al. (2015)
		Nov 2011—Mar 2012 (*n* = 23) — MBB [b]	47—240 h	Spring & Summer	Marine/Continent	
Rio de Janeiro (Rio J., Brazil)	PM$_{2.5}$	Jan 2015 (*n* = 3)	24 h	Summer	Marine	This study
	PM$_{10}$	Jan 2015 (*n* = 4)			Marine	
São Paulo (S. Paulo, Brazil)	PM$_{10}$	Jan—Mar 2014 (*n* = 8)	24 h	Summer	Marine	This study
		July—Sept 2014 (*n* = 7)		Winter	Continent	
Aveiro (Portugal)	PM$_{2.5}$	July—Aug 2010 (*n* = 3)	168 h	Summer	Marine	Lopes et al. (2015)
		Dec 2010—Feb 2011 (*n* = 5)		Winter	Marine/Continent	
Lisbon (Portugal)	PM$_{2.5}$	July—Sept 2013 (*n* = 8)	96 h	Summer	Marine/Continent	This study

[a] *n* = Number of aerosol samples.
[b] IBB — Intense Biomass Burning, MBB — Moderate Biomass Burning.
[c] Origin of air masses during each sampling period, based on air mass back trajectories assessed by means of the HYSPLIT model, using the Global Data Assimilation System (GDAS) meteorological database, and accessed via NOAA Air Resources Laboratory READY website (Draxler and Rolph, 2014; Rolph, 2014).

collect enough material for subsequent WSOC characterization. Additional details on aerosol sampling procedure in Aveiro are available in section S1, in SI.

The capital city of Portugal, Lisbon, is the westernmost capital in mainland Europe, and it is set at the north of the Tagus estuary and in close proximity to the Atlantic Ocean. It is the largest urban area in Portugal with a population of about 2.8 million. Although there is some industrial activity, the traffic is the main source of local atmospheric emission. In addition, the international airport located in the north of the city is also a significant contributor to local emissions. In Lisbon area, the aerosol sampling was carried out at the Laranjeiro Air Quality Station, approximately 4 m above the ground. A total of eight 96 h high-volume PM$_{2.5}$ samples were collected on 150 mm i.d. quartz fibre filters (Whatman QM-A), during July—September 2013. Additional details on aerosol sampling are available in section S1, in SI.

Samples from Buenos Aires, Medellín, Bogotá, and Lima were collected during the development of South American Emissions, Megacities and Climate Project (SAEMC). The objectives of this

project were to provide accurate regional emissions and climate change scenarios for South America, with emphasis on the impacts of and on megacities. In Medellín, the second biggest city in Colombia (2.3 million inhabitants, data from the National Department Administrative of Statistics of Colombia), the sampling was done in a monitoring zone (Poblado), near to an avenue with heavy traffic (1955 vehicles per hour). Twelve 24 h PM$_{10}$ samples were collected on quartz fibre filters (20.3 × 25.4 cm; Whatman QM-A), between June 16th and 28th (2008), during the dry season. In Bogotá, capital of Colombia, with approximately 8 million inhabitants and about 1.2 million vehicles, twelve 24 h PM$_{10}$ samples were collected from November 24th to December 9th (2008), during the wet season, on quartz fibre filters (20.3 × 25.4 cm; Whatman QM-A), at a site with strong vehicular emissions. Additional details on aerosol sampling in Bogotá can be found in the study of Vasconcellos et al. (2011). At Buenos Aires (14 million inhabitants in the metropolitan area), Argentina, thirteen 24 h PM$_{10}$ samples were collected from August 14th to September 15th (2008), on quartz fibre filters (20.3 × 25.4 cm; Whatman QM-A).

The aerosol sampling was carried out on a rooftop (approximately 12 m above the ground) of a building at Comisión Nacional de Energía Atómica, over 15 m distance from a highway. The sampling site is mainly influenced by residential and vehicular emissions (Vasconcellos et al., 2011). In Lima (8.5 million inhabitants; data from the National Statistical System of Peru), capital of Peru, the sampling campaign was carried out in Campo de Marte, the biggest urban park, localized in the central region of the city. Ten 24 h PM_{10} samples were collected from June 17th to August 11th (2010), on quartz fiber filters (20.3 × 25.4 cm; Whatman QM-A, NP, 1851-865). Additional details on aerosol sampling in Buenos Aires, Medellín, Bogotá, and Lima are available in section S1, in SI.

In Brazil, sampling of aerosols was carried out at three different locations: Porto Velho (PV), São Paulo (S. Paulo), and Rio de Janeiro (Rio J.). In PV, the PM_{10} samples were collected in a forest reserve located about 5 km of Porto Velho, in the state of Rondônia, western Amazon. In contrast to urban areas, where air pollution sources are independent of climate seasonality, biomass burning in the Amazon region occurs mainly during the dry season (July–October), when the highest inflammability of the forest is observed. Therefore, in PV, the aerosol sampling was carried out during two well distinct periods: the dry season (August–October 2011) and the wet season (November 2011–March 2012). Given the distinct strength of the biomass burning events, the former will be referred hereafter as intense biomass burning (IBB) whereas the latter as moderate biomass burning (MBB) periods. The high-volume sampler was deployed at a site close to the dense forest, and the PM_{10} samples were collected on quartz fiber filters (20.3 × 25.4 cm; Energética) (De Oliveira Alves et al., 2015). After sampling, the PM_{10} samples were kept at 4 °C covered in aluminum during the field campaigns. The refrigerator was placed in a container located on the border of a 150 m radius grassland clearance at the south-west corner of 2000 ha of the dense forest. As described in a previous study of De Oliveira Alves et al. (2015), the average concentrations of PM_{10} during IBB and MBB periods were 30.2 ± 12.3 μg m^{-3} and 13.4 ± 3.15 μg m^{-3}, respectively. Peak concentration of PM_{10} during IBB was observed to reach 60 μg m^{-3} on the 24 h average (De Oliveira Alves et al., 2015). At S. Paulo, the PM_{10} samples were collected on quartz fiber filters (20.3 × 25.4 cm; Energética), during an extensive campaign carried out in January–March 2014 [$n = 8$, Summer (SU) period] and July–September 2014 [$n = 7$, Winter (WI) period]. In Rio J., 24 h high-volume $PM_{2.5}$ ($n = 3$) and PM_{10} ($n = 4$) samples were simultaneously collected on quartz fibre filters (20.3 × 25.4 cm; Whatman QM-A) during January 2015. The sampling occurred at the Campus of the Pontifical Catholic University of Rio de Janeiro, on a rooftop approximately 39 m above the ground. The sampling site is located on the east coast of Brazil, 2 km from the Atlantic Ocean, nearby a heavy traffic street, and only a few meters away from a subway line construction. The sampling area is also surrounded by the Tijuca Forest. The high-volume $PM_{2.5}$ and PM_{10} samplers were installed on platforms (1 m high from the rooftop), with a distance of approximately 2 m from each other in order to avoid any interference. Additional details on aerosol sampling at the different Brazilian sites are available in section S1, in SI.

All quartz filters used in the aforementioned sampling campaigns were previously heated (at 500 °C or 800 °C for 12 h or 8 h, respectively) in order to remove any organic contaminants. The total mass of each collected aerosol sample was determined by weighing the filter under controlled moisture conditions before and after sampling (see section S1 in SI for further details). The ambient PM_{10} and $PM_{2.5}$ concentrations are expressed in μg m^{-3}. The filters were then wrapped with aluminum foil and stored frozen until further analysis.

2.2. Extraction and determination of WSOC in aerosol samples

Depending on the available filter area, the volume of ultra-pure water used for extraction the WSOC had to be adjusted in order to comply with a "filter area-to-water volume ratio" between 1.0 and 3.5 cm^2 mL^{-1}. For the aerosol samples collected in Aveiro and Rio J., each quartz filter was extracted with 150 mL of ultra-pure water (18.2 M Ω cm) by mechanical stirring for 5 min followed by ultrasonic bath for 15 min. This same extraction methodology was applied to the other aerosol samples (Lisbon, Medellín, Bogotá, Buenos Aires, Lima, PV, and S. Paulo) using a volume of ultra-pure water of 50 mL. Each final obtained aqueous slurry was filtered through a hydrophilic polyvinylidene fluoride (PVDF) membrane filter (Durapore®, Millipore, Ireland) of 0.22 μm pore size. The dissolved organic carbon (DOC) content of each aqueous aerosol extract of samples collected in Aveiro and Lisbon was measured by means of a Shimadzu (Kyoto, Japan) TOC-5000A Analyzer, using the non-purgeable organic carbon (NPOC) method (Lopes et al., 2015), whereas the DOC content of the aqueous extracts of aerosol samples collected in South America locations was measured with a Skalar (Breda, Netherlands) San++ Automated Wet Chemistry Analyzer, based on a UV-persulfate oxidation method. It should be emphasized that both high-temperature combustion and wet oxidation methods perform at a relatively satisfactory level and there is no evidence for systematic differences on the DOC content derived from the two methods, as demonstrated in a previous work by Lopes et al. (2006). The WSOC concentrations are expressed in μg C m^{-3}.

After WSOC extraction, and to ensure enough mass for the structural characterization, the aqueous extracts were batched together according to the groups representative of each urban location and/or season or sampling condition, as outlined in Table 1. For the particular case of the aerosol WSOC samples collected in Aveiro and Lisbon, each pooled WSOC sample was further isolated/fractionated by adsorption onto a Supelite™ DAX-8 resin, following a well-established analytical protocol (Duarte and Duarte, 2005; Duarte et al., 2007). This isolation procedure was employed under the framework of a previous study where the water-soluble organic functionality of the urban aerosol samples was investigated using solid-state ^{13}C NMR and Fourier Transform Infrared (FTIR) spectroscopies (Duarte et al., 2015). Therefore, the structural characterization of the samples collected in Aveiro and Lisbon presented in Section 3 comprises the WSOC fractions recovered from the resin, as these fractions accounts for 42–53% of the total DOC of the aqueous extracts, and contains the highest percentages of chromophoric compounds (60–67% of the total UV absorbance at 250 nm of the aqueous extracts, data not shown) (Lopes et al., 2015). Finally, each pooled WSOC sample analyzed in this study, including the isolated WSOC fractions from Aveiro and Lisbon, was concentrated under rotary evaporation followed by a freeze drying procedure, and kept on a desiccator over silica gel until ^{1}H NMR analysis.

2.3. Solution-state ^{1}H NMR spectroscopy

All ^{1}H NMR spectra were acquired on a Bruker Avance-500 spectrometer operating at 500.13 MHz, equipped with a liquid nitrogen cooling CryoProbe. All spectra were run at 22 °C, under the following conditions: i) pulse with of 3.83 ms; b) acquisition time of 2.97 s; c) 64 k data points; d) spectral with of 11029 Hz; e) recycle delay of 1 s; and f) 1024 scans. The dried WSOC samples were dissolved in deuterated methanol (MeOH-d_4, 1 mL) and transferred to 5 mm NMR tubes. The identification of functional groups in the ^{1}H NMR spectra was based on their chemical shift relative to that of an internal tetramethylsilane (TMS) standard set at 0 ppm.

3. Results and discussion

3.1. Contribution of WSOC to PM mass

Table 2 reports the range of ambient concentrations of PM, WSOC, total mass of particulate water-soluble organic matter (WSOM), and percentage of mass ratio between WSOM and PM at each studied location. The total mass of WSOM was estimated as $1.6 \times$ WSOC, based on elemental analysis performed on the WSOC aerosol samples collected at Aveiro (Duarte et al., 2015). In Aveiro, this factor ranged between 1.5 in winter and 1.7 in summer, yielding an average WSOM–to–WSOC ratio of 1.6 (Duarte et al., 2015). It is very likely that this ratio would vary from site to site. In Bogotá, Vargas et al. (2012) used 1.6 and 1.8 to convert organic carbon-to-organic material with good PM_{10} mass closure results. Due to the lack of additional information for the remaining locations focused in this study, a value of 1.6 was used here to calculate the total mass of particulate WSOM at all sites.

As depicted in Table 2, the highest median values of the WSOM/PM ratio are found in Aveiro (7.2 and 21% in SU and WI, respectively), Lisbon (6.7%), and Rio J. (8 and 13% for PM_{10} and $PM_{2.5}$, respectively), suggesting that OA in these locations might be dominated by more processed oxygenated (therefore, more water-soluble) organic structures. In contrast, for the South American sites of Medellín, Bogotá, Buenos Aires, Lima, PV, and S. Paulo, the median values of the WSOM/PM ratios remain rather similar and below 1.3%. One of the notable features observed in this study is the apparent insignificant site-to-site variation in terms of solar radiation, ambient temperature, and relative humidity, especially during warmer conditions (Table S1, in SI). This would be indicative of exceptional atmospheric conditions for attaining similar amounts of secondary organic components across the different European and South American locations. However, the observed low WSOM/PM ratios (<1.3%) may be explained by the significant presence of apparently chemically reduced OA probably related to freshly emitted traffic aerosols in Medellín, Bogotá, Buenos Aires, Lima, PV, and S. Paulo (Vasconcellos et al., 2011). Also of note, Bogotá presents the lowest median value for the WSOM/PM ratio among the South American sites. This outcome could be due to a combination of various controlling factors, including meteorological events (e.g., highest amount of total precipitation, Table S1 in SI) and higher contribution of direct vehicular emissions to the aerosol OC fraction, particularly when compared to the cities of S. Paulo and Buenos Aires, where it has been suggested that secondary photochemical production of OC seems to be more important (Vasconcellos et al., 2011). Also noteworthy is the higher median WSOM/PM ratio observed in PV (within the Brazilian Amazon region) during IBB events as compared to that observed during MBB events. A source apportionment study carried out during these two events have shown that biomass burning is the larger contributor to aerosol OC load in this sampling region (De Oliveira Alves et al., 2015). Previously, Mayol-Bracero et al. (2002) have also provided strong evidences that aerosol WSOC is generated in significant amounts during biomass burning within this region, thus explaining the WSOM/PM ratios (Table 2) determined during the IBB and MBB sampling periods.

Data reported in Table 2 for Rio J. during summer, also shows that WSOC is enriched in $PM_{2.5}$ samples (range of $PM_{2.5}/PM_{10}$ ratios = 62–80%). The SOA and biomass burning particles are main contributors to WSOC and both are known to be preferentially associated with the $PM_{2.5}$ size fraction (e.g. Fuzzi et al., 2007). From a seasonal standpoint, at Aveiro, the WSOM contributes to 13–32% of the PM mass during winter, whereas its contribution diminishes during summer to 5.7–10%. Apparently, in S. Paulo, the lowest levels of the WSOM/PM ratios were also observed during summer season, although no variation between seasons could be discern based on the obtained median WSOM/PM values. These results suggest that contributions of biomass burning combined with low temperature conditions (average value of 11 °C, Table S1 in SI) could be important to ambient water-soluble OA in Aveiro during winter (e.g., Duarte et al., 2015), whereas the somewhat lower relative humidity and total precipitation and higher ambient temperatures (average value of 17 °C) in S. Paulo during winter (Table S1 in SI) could contribute to the observed range of WSOM/PM ratios.

3.2. Proton (^1H) functional group characteristics

Fig. 2 shows the ^1H NMR spectra of WSOC fractions extracted from the atmospheric PM samples collected at each studied location. Before going deeper inside the wealth of structural information provided by these NMR spectra, it must be emphasized that the spectra of the WSOC samples collected in Aveiro and Lisbon are significantly better resolved in terms of sensitivity than those of the South America samples. The most plausible explanation for this low spectrum intensity is related to the low dissolved carbon content of the South America samples as compared that of the Western European samples, particularly because the latter has been subjected to an isolation (and concentration) procedure onto DAX-8 resins

Table 2
Range of ambient concentrations of PM, WSOC, total mass of particulate water-soluble organic matter (WSOM), and percentage of mass ratio between WSOM and PM (median values are given in parentheses; ± standard deviation) at each studied location.

Location/Sample	Total PM ($\mu g\ m^{-3}$)	WSOC ($\mu g\ C\ m^{-3}$)	WSOM [c] ($\mu g\ m^{-3}$)	WSOM/PM (%)
Medellín	10.9–59.4	0.05 ± 0.01–0.34 ± 0.01 (0.11 ± 0.01)	0.087–0.55 (0.18 ± 0.02)	0.24–2.5 (0.43)
Bogotá	23.6–48.9	0.04 ± 0.009–0.13 ± 0.01 (0.08 ± 0.01)	0.062–0.21 (0.13 ± 0.01)	0.16–0.67 (0.35)
Lima	33.5–59.1	0.27 ± 0.01–0.38 ± 0.01 (0.33 ± 0.01)	0.43–0.61 (0.53 ± 0.02)	1.0–1.4 (1.3)
Buenos Aires	14.5–160	0.07 ± 0.003–4.7 ± 0.31 (0.11 ± 0.01)	0.11–7.6 (0.18 ± 0.01)	0.11–16 (0.49)
PV – IBB [a]	13.1–58.6	0.01 ± 0.01–0.43 ± 0.01 (0.18 ± 0.01)	0.15–0.69 (0.29 ± 0.01)	0.89–1.4 (1.2)
PV – MBB [a]	9.46–18.3	0.029 ± 0.001–0.10 ± 0.01 (0.054 ± 0.004)	0.046–0.16 (0.09 ± 0.001)	0.39–1.2 (0.66)
Rio J. – $PM_{2.5}$	10.6–22.1	0.83 ± 0.02–1.3 ± 0.1 (1.0 ± 0.1)	1.3–2.1 (1.6 ± 0.1)	6.0–16 (13)
Rio J. – PM_{10}	26.4–46.0	1.3 ± 0.1–1.8 ± 0.1 (1.6 ± 0.1)	2.1–2.9 (2.5 ± 0.1)	5.7–8.4 (8.0)
S. Paulo – SU [b]	20.7–164	0.07 ± 0.003–0.28 ± 0.01 (0.12 ± 0.05)	0.11–0.44 (0.19 ± 0.08)	0.11–1.2 (0.58)
S. Paulo – WI [b]	33.5–113	0.10 ± 0.01–0.45 ± 0.01 (0.32 ± 0.16)	0.16–0.72 (0.51 ± 0.26)	0.39–1.2 (0.56)
Aveiro – SU [b]	20.5–27.0	0.37 ± 0.03–0.99 ± 0.06 (0.65 ± 0.04)	0.59–1.6 (1.0 ± 0.1)	5.7–10 (7.2)
Aveiro – WI [b]	14.5–37.0	1.8 ± 0.1–5.0 ± 0.1 (2.9 ± 0.1)	2.9–7.9 (4.6 ± 0.1)	13–32 (21)
Lisbon	25.5–95.5	0.95 ± 0.01–5.7 ± 0.1 (2.0 ± 0.1)	1.5–9.2 (3.2 ± 0.1)	4.7–9.6 (6.7)

[a] IBB – Intense Biomass Burning, MBB – Moderate Biomass Burning.
[b] SU – Summer season, WI – Winter season.
[c] [WSOM] = [WSOC] × 1.6 (factor used to convert WSOC into WSOM derived from elemental analysis on WSOC aerosol samples collected at Aveiro (Duarte et al., 2015)).
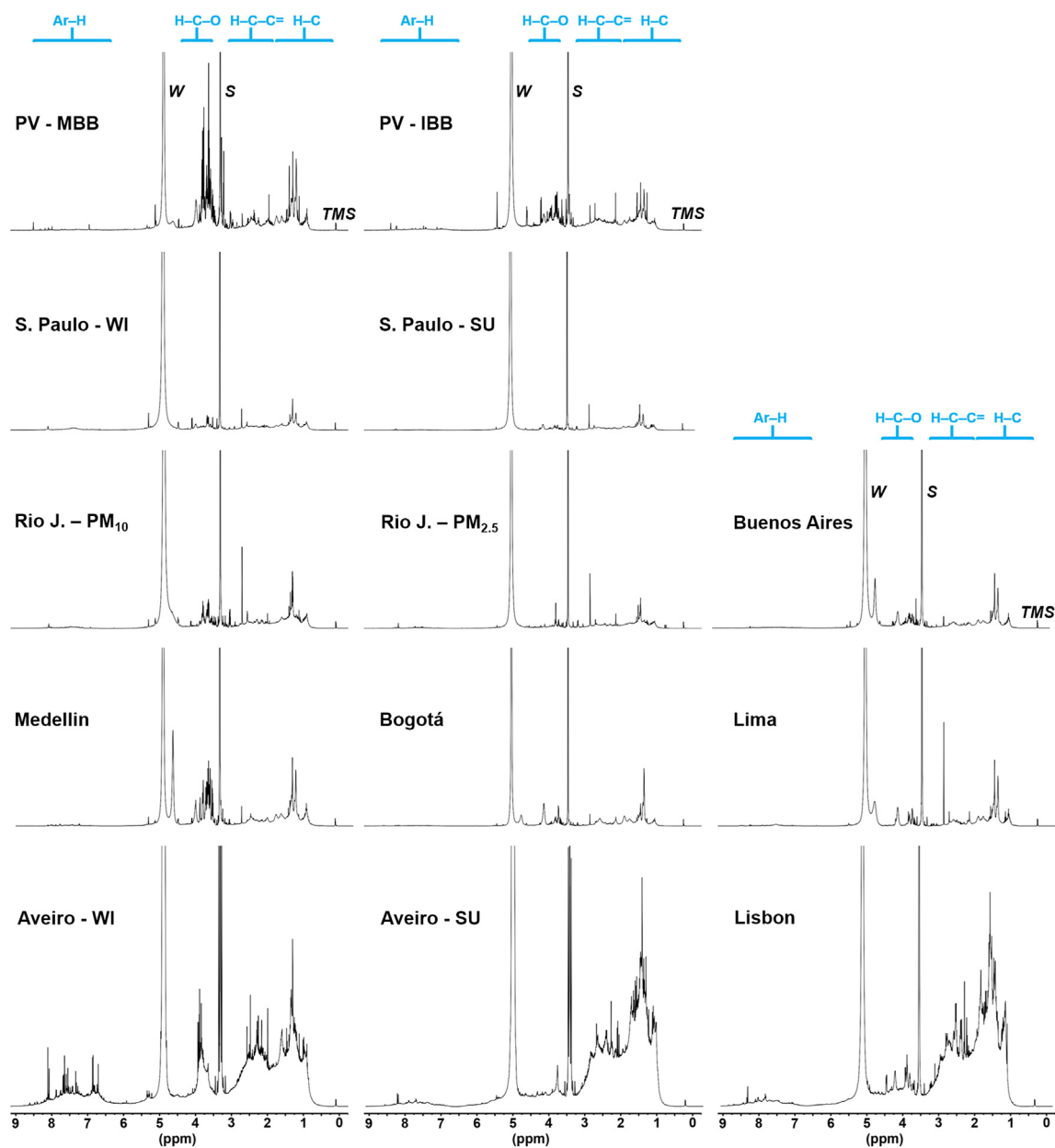
Fig. 2. Solution-state ^{1}H NMR spectra of WSOC from the aerosol samples collected at the different South America and Western European sites. Four spectral regions are identified (in blue) at the top of the spectra: H–C, H–C–C=, H–C–O, and Ar–H. Resonance signals: Water (W), Solvent (S) – MeOH-d_4, and Tetramethylsilane (TMS) – 0.03% (v/v). Sampling periods and samples identification are given in Tables 1 and 2, respectively. (For interpretation of the references to colour in this figure legend, the reader is referred to the web version of this article.)

(see section 2.2). As recently demonstrated by Lopes et al. (2015), this isolation procedure is unlikely to exert a bias in WSOC composition and, therefore, affect the comparison between the ^{1}H NMR profiles of the isolated and non-isolated WSOC samples. It has been also shown that the isolated WSOC samples can be considered as good proxies of the total aerosol WSOC (Lopes et al., 2015).

The most distinct feature of the aerosol WSOM spectra is that the majority of the NMR signals remain unresolved and superimposed by a relatively small number of sharp peaks, suggesting the occurrence of complex mixtures of organic structures. In this scenario, the identification of specific individual organic species becomes difficult, although four main categories of functional groups carrying C–H bonds can be identified: (i) δ [1]H 0.5–1.9 ppm – protons bound to carbon atoms of straight and branched aliphatic

chains (H-C), which includes protons from methyl (R–CH$_3$), methylene (R–CH$_2$), and methyne (R–CH) groups; (ii) δ [1]H 1.9–3.2 ppm – protons bound to carbon atoms in α–position to unsaturated groups in allylic (H–C$_\alpha$–C=), carbonyl or imino (H–C$_\alpha$–C=O or H–C$_\alpha$–C=N) groups, protons from methyl groups bound to an aromatic carbon, and protons in secondary and tertiary amines (H–C–NHR and H–C–NR$_2$); (iii) δ [1]H 3.5–4.1 ppm – protons bound to oxygenated saturated aliphatic carbon atoms (H–C–O) in alcohols, polyols, ethers, esters, and organic nitrate (R–CH$_2$–O–NO$_2$), and (iv) δ [1]H 6.5–8.3 ppm – protons bound to aromatic carbon atoms (Ar–H). For a further understanding of the ^{1}H NMR spectra profiles, a quantitative integration of each spectral region was performed in order to assess the abundance of each functionality in the WSOM samples. As depicted in Fig. 3, regardless
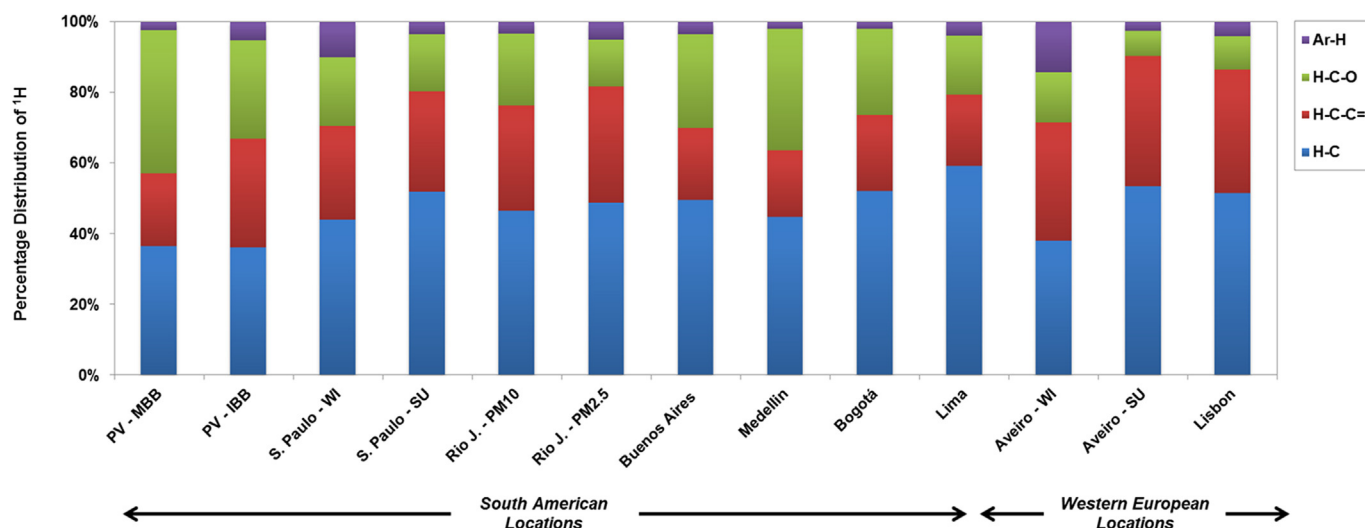
Fig. 3. Percentage distribution of ^{1}H NMR in WSOC from the aerosol samples collected at the different South America and Western European sites. Sampling periods and samples identification are given in Tables 1 and 2, respectively.

of the studied environment, all aerosol WSOC samples exhibit the same major proton types; however, they differ in terms of the relative distribution of the major proton regions. Overall, the relative content of the proton functional groups obtained in this study are within the range of those published for WSOC hydrophobic acid fractions or "humic-like substances (HULIS)" from atmospheric aerosols (e.g., Graham et al., 2002; Decesari et al., 2005; Song et al., 2012; Chalbot et al., 2014, 2016; Lopes et al., 2015). For the South American sites, the saturated aliphatic protons are the most important component (36–59%), followed by unsaturated (20–33%) and oxygenated (13–40%) aliphatic protons, and a less contribution from aromatic protons (2.0–10%). In a similar fashion, for the WSOC samples collected in Western Europe, the relative contributions of these four proton functional groups vary in the following order: H-C (38–53%) > H–C–C= (33–37%) > H-C-O (7.0–14%) > Ar-H (2.7–14%). However, a different trend is observed for samples collected in PV during MBB, Medellín, Bogotá, and Buenos Aires, for which the relative contribution of H-C-O structures (40%, 34%, 24%, and 27%, respectively) surpasses that of the H-C-C= structures (21%, 19%, 21%, and 20%, respectively). Examples of organic species that typically resonate in this region includes not only sugar alcohols (e.g., mannitol and arabitol), but also other carbohydrate-like moieties such as glucose, sucrose, and fructose (Chalbot et al., 2014), as well as anhydrosugars, such as levoglucosan and mannosan (Duarte et al., 2008). Sugar alcohols are particularly widespread in fungi and have been proposed as molecular tracers for fungal spores in ambient aerosol (e.g., Bauer et al., 2008; Fu et al., 2010; Liang et al., 2013). Nevertheless, other sources of sugar alcohols in airborne PM cannot be excluded, such as vegetation during springs blossoms and decomposing plants during cold seasons (Burshtein et al., 2011). Primary saccharides can also have a biological origin (e.g., Fu et al., 2010), whereas anhydrosugars are mainly associated with the emissions from biomass burning (e.g., Duarte et al., 2008; De Oliveira Alves et al., 2015). Therefore, the predominance of the H-C-O signature in the aforementioned WSOC samples could be associated with the presence of primary biogenic material (e.g., pollen and fungal spores) with an important carbohydrate signature. In this regard, the portion of spores in PM_{10} in Amazonia has been estimated to be 25% during day time and 45% at night, with an average of 35% (Elbert et al., 2007). Additionally, the NMR spectra (Fig. 2) of the WSOC samples collected in PV - MBB, Medellín, Bogotá, and Buenos Aires

exhibit two distinct peaks at δ ^{1}H 3.98 and 4.61 ppm, which are likely assigned to the protons in the H-O- groups of a sugar alcohol skeleton, thus supporting the contribution of fungal spores and pollen into the water-soluble OA composition at these locations. Nevertheless, H-C-O structures in PV − MBB and Bogotá may also have a secondary origin, as a result of photochemical reactions (e.g., stronger solar radiation in Bogotá, Table S1), and/or atmospheric aging of primary OA during warmer conditions (e.g., average temperature of 26 °C in PV − MBB, Table S1) (Shakya et al., 2012; Chalbot et al., 2016). The strong H-C-O signature in the NMR spectra of samples from Medellín and Buenos Aires during winter and winter/spring seasons, could also be attributed to the presence of carbohydrate-like moieties likely derived from plant cellulose and hemicellulose pyrolysis, which underpins the contribution of biomass burning emissions to the urban OA. In the particular case of Medellín, the sampling campaign occurred under the influence of transported biomass burning emissions taking place in Amazonia at that same time. In addition, the NMR spectra of the Medellín and Buenos Aires samples exhibit a peak at δ ^{1}H 5.3 ppm, assigned to anhydrosugars from cellulose, such as levoglucosan and mannosan (Duarte et al., 2008), further corroborating the contribution of biomass burning into the OA composition.

The potential contribution of fresh biomass burning compounds to WSOC during winter can also be inferred from the highest aromatic content of the samples collected in Aveiro (14%) and S. Paulo (10%) as compared to those collect in summer (2.7 and 3.5%, respectively) at the same urban locations. Also, the presence of an intense sharp resonance at δ ^{1}H 5.3 ppm attributed to anhydrosugars in these samples further confirms the presence of smoke particles during this period. Nonetheless, one cannot rule out that in S. Paulo, the aromatic structures could also originate from traffic sources, especially, from diesel and gasoline emissions (Agudelo-Castañeda and Teixeira, 2014). Unsurprisingly, WSOC collected in PV during the IBB period exhibit a clear biomass burning assignment, with a higher aromatic content (5.2%) and an intense NMR signal from anhydrosugars than WSOC collected during the MBB event (2.4%). These results agree with those described by De Oliveira Alves et al. (2015) for the same location and sampling period, where levoglucosan was observed in significant concentrations and biomass burning was found to be the dominating aerosol source. Inversely, these same group of authors reported that PM_{10} was relatively constant throughout the MBB event, suggesting

an overall stable balance between aerosol sources and sinks within the filter sampling resolution.

Also interestingly, the WSOC from PM$_{2.5}$ samples collected during summer in Rio J., Aveiro, and Lisbon exhibit a proton functional group composition compatible with SOA formation, all holding similar relative content of H-C, H-C-C=, and H-C-O (49—53%, 33—37%, and 7—13%, respectively). However, the relative content of aromatic protons in summer WSOC in Aveiro is lower (2.7%) than those in Rio J. and Lisbon (5.1 and 4.1%, respectively). As aforementioned, the aromatic moieties could also be associated with emissions from anthropogenic activities, which are expectedly to be more enhanced in large cities such as Rio J. and Lisbon. In Lima, Peru, a location characterized by low rainfall rates (Table S1, in SI), the saturated and unsaturated aliphatic moieties dominate the average chemical structure of WSOC PM$_{10}$ samples during winter, which may imply the potential contribution of combustion sources.

Aiming at attain additional details on the structural differences between the aerosol WSOC samples with respect to the different studied scenarios, each main category of proton functional groups has been further divided into recognizable ^{1}H NMR resonances associated with specific key structural units, which are summarized in Table 3. These assignments are based on the structural information provided by two-dimensional NMR studies of aerosol WSOC reported in a previous study (Duarte et al., 2008). A quantitative integration of each spectral region has been also performed in order to assess the abundance of each structural unit in the WSOC samples. The radar diagram shown in Fig. 4 indicates that the region of saturated (δ ^{1}H 0.5—1.9 ppm) and unsaturated (δ ^{1}H 1.9—3.2 ppm) aliphatic protons, which are major contributors to WSOC composition, maintain their overall characteristics across the different WSOC samples. A large proportion of these aliphatic NMR resonances is likely to be represented by terminal methyl groups (16—26%) in long-chain (carbons greater than 3 or 4) and/or branched functionalized structures with a heteroatom 4 bonds away from protons (12—21%). The abundance of the so-defined unsaturated aliphatics is governed by protons located 3 bonds away from a heteroatom (δ ^{1}H 2.2—3.2 ppm; 13—25%), being the carboxylic group the most likely substitution pattern. The WSOC samples from Lima, Bogotá, and S. Paulo − SU are particularly

enriched in methyl groups (23—26%, δ ^{1}H 0.5—1.3 ppm), whereas summer WSOC in PM$_{2.5}$ from Aveiro, Lisbon, and Rio J. present the highest values (42—46%) for the relative content of functionalized aliphatics with a heteroatom 3 to 4 bonds away from protons (δ ^{1}H 1.4—1.9 ppm plus δ ^{1}H 2.2—3.2 ppm). These latter features are, in general, likely compatible with an enhanced SOA formation during summer at these locations. These functionalized structures are much less abundant (27%) in WSOC collected in PV samples during MBB and in Medellín.

The major differences between the WSOC samples are verified within the carbohydrate-like and aromatic moieties. The WSOC samples from Aveiro and Lisbon seem to be somewhat depleted in carbohydrate-like moieties (NMR resonance at δ ^{1}H 3.5—3.9 ppm), particularly when compared to WSOC samples from South America. This feature might be an artifact of the Aveiro and Lisbon samples preparation as DAX-8 resin could discriminate against carbohydrates (Fan et al., 2013). Notwithstanding this fact, and regardless of the studied environment, H-C-O groups from carbohydrates (e.g., proton bound to carbon C$_6$ in CH$_2$-O groups) are likely to represent the most important contribution to the singly oxygenated structures present in the studied WSOC samples. The highest relative contributions were found for WSOC collected in PV during MBB (33%) and in Medellín (28%). In both cases, this structural signature could have a biogenic origin (e.g., atmospheric pollen, fungal spores, and decomposing plants). The impact of smoke particles can also explain the important contribution (21%) of this structural signature for the aerosol WSOC in PV during IBB. Among the two Western European cities, the smoke impacted winter Aveiro sample also exhibit the highest abundance of carbohydrate-like moieties (9.0%). Within the H-C-O chemical shift section, the structural signature likely assigned to polyols, such as sugar alcohols (NMR resonance at δ ^{1}H 3.9—4.1 ppm), appears to be most abundant for Bogotá (12%), Buenos Aires (9.3%), and Lima (8.0%) samples. As aforementioned, the presence of sugar alcohols in air particles could be associated with the contribution of fungal aerosols and/or decomposing plants, whose levels are expected to be high during spring/summer and winter/spring periods (coincident with the sampling periods in Bogotá and Buenos Aires, respectively). Polyols are also traditionally identified as marker compounds for the photooxidation of isoprene in aerosols (e.g., 2-methyltetrols) (Fu

Table 3
Description of ^{1}H NMR key structural units identified in the WSOC fractions extracted from the aerosol samples collected at different locations from South America and Western Europe. The interacting proton is highlighted in bold.

| Main structure	Code	δ (^{1}H) [ppm]	Key structural units
H-C	**AL - 1**	0.5 −1.3	Terminal C**H$_3$** groups in aliphatic chains, and in certain branched aliphatics CCCC**H**; C**H$_3$** groups as substituent in aromatic structures (δ$_H$ ≈ 1.2 ppm)
	AL - 2	1.3 −1.4	Mid-chain C**H$_2$** groups in aliphatic structures at more than 3 or 4 bonds from -COOH, -OH or NH$_2$ functionalities
	AL - 3	1.4 −1.9	C**H$_2$** or C**H** groups in aliphatic (some branched) structures β to a -COOH, -OH or NH$_2$ functionality
H-C$_\alpha$-C=	**AL - 4**	1.9 −2.2	Acetate group (**H**$_3$C-COO-R); C**H** groups in branched aliphatic structures α to a -COOR functionality
	AL - 5	2.2 −3.2	C**H$_2$** or C**H** groups in aliphatic structures α to -COOH (δ$_H$ ≈ 2.3 ppm), -C=O or -NH functionality (δ$_H$ > 2.5 ppm), and/or in β position to -COOR functionality (at δ$_H$ > 2.5 ppm); C**H$_3$** groups as substituent in aromatic structures (δ$_H$ ≈ 2.3 or 2.5 ppm) or in **H**$_3$C-C(O)-R aliphatic structures (δ$_H$ ≈ 2.3 ppm)
H-C-O	**O-AL-1**	3.5 −3.9	Mostly C**H$_2$**-OH groups (C$_6$ carbon) from carbohydrates, and in a less extent oxymethylene (-OC**H$_2$**-O-; δ$_H$ ≈ 3.6—3.7 ppm) units, and C**H$_3$** groups in aromatic (R$_{ar}$-COOC**H$_3$**) and aliphatic (R$_{al}$-COOC**H$_3$**) methyl esters, and aromatic methyl ethers (R$_{ar}$-OC**H$_3$**)
	O-AL-2	3.9 −4.1	-C-C**H**-OH groups from polyols (δ$_H$ ≈ 4.0 ppm)
Ar-H	**AR - 1**	6.5 −7.1	Aromatic protons with -OH or methyl ethers (-OCH$_3$) substituents in the neighboring aromatic carbon
	AR - 2	7.1 −8.0	Aromatics with alkyl, oxygenated alkyl, -OR, methyl ethers (-OC**H$_3$**), -COOH, and/or nitrite (NO$_2$) substituents
	AR - 3	8.0 −8.3	Oxidized aromatics, mainly (poly)carboxylated aromatics (e.g., terephthalic acid)
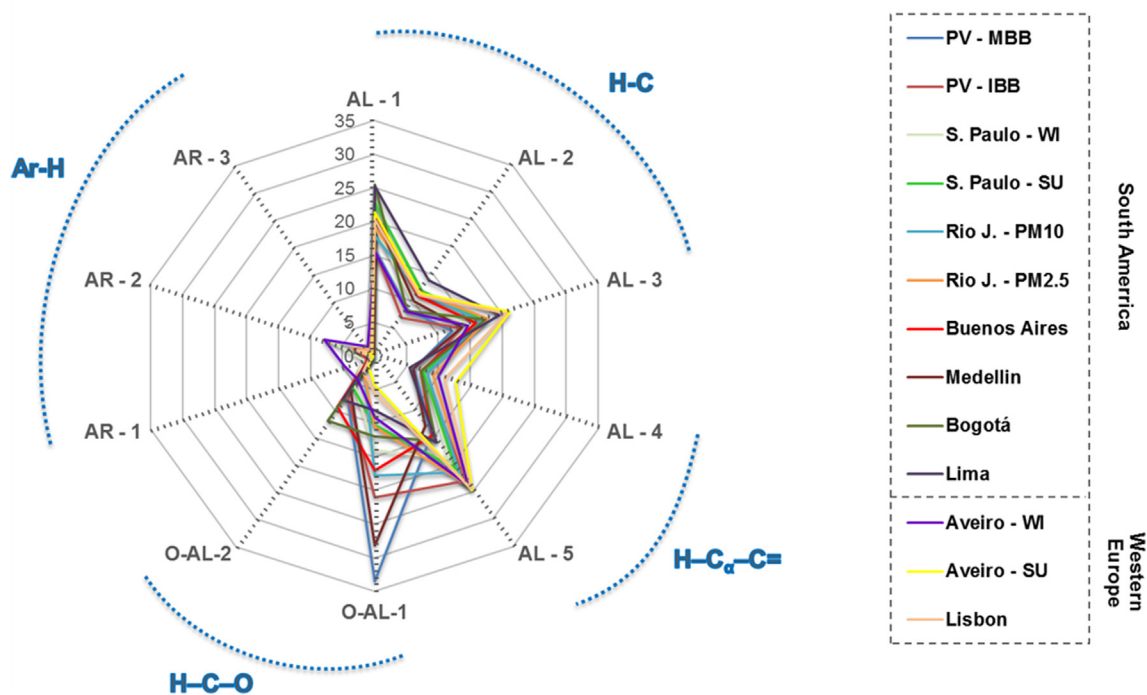
Fig. 4. Radar diagram of the ^{1}H NMR section integrals, derived from total area-normalized ^{1}H NMR spectra integrals according to structural zones depicted in Table 3 (see Table 3 for the attribution of δ ^{1}H section integrals and codes), for all aerosol WSOC samples collected at the different South America and Western European sites. Sampling periods and samples identification are given in Tables 1 and 2, respectively.

et al., 2010; Minguillón et al., 2016). The presence of such secondary products derived from the oxidation of biogenic volatile organic compounds have already been reported for urban OA in tropical India (Fu et al., 2010) and Barcelona (Minguillón et al., 2016). Thus, the presence of biogenic SOA tracers in Bogotá and Buenos Aires WSOC samples cannot be ruled out. During winter, coincident with the sampling period in Lima, different sources of fungal spores could also contribute to the presence of sugar alcohols, such as the resuspension from exposed surfaces (e.g., soil resuspension) and decomposing plants. It should be emphasized that the presence of fungal spores in urban areas is not uncommon - recently, Liang et al. (2013) have reported a high abundance of fungal spores in an urban area in Beijing (China). As fungal spores and related chemical components have been associated with adverse health effects, their presence in South America (mega)cities should cause further environmental and public health concerns.

Most of the aromatic structures were found in the chemical shift region δ [1]H 7.1–8.0 ppm (Fig. 4), which was indicative of aromatic structures with a diverse suite of different substituents (see Table 3). In WSOC samples collected during winter seasons, such as those from PV during IBB, S. Paulo, Buenos Aires, Lima, or Aveiro, these type of structural features are probably matching the presence of breakdown products resulting from the pyrolysis of lignin, such as phenols, aldehydes, ketones, acids, and alcohols, generally with the same substituent pattern on the aromatic rings as the precursor aromatic alcohols from which they were derived (Duarte et al., 2008). Once in the atmosphere, these structures can also undergo photooxidation, originating highly oxidized aromatic SOA species (Iinuma et al., 2010). Nevertheless, other aromatic structures with a secondary origin can resonate in this NMR region, such as terephthalic acid, nitrophenyl-derived compounds, cinnamic acid and/or cinnamaldehyde, possibly formed during the oxidation of aromatic hydrocarbons from urban traffic emissions (Hallquist

et al., 2009; Chalbot et al., 2014; Lee et al., 2014).

3.3. Source apportionment of aerosol samples

In order to assess if the proton functional group distribution could shed light on the dominant particulate WSOC sources at each site, the source apportionment technique developed by Decesari et al. (2007) was applied to all samples. By plotting the ratios of calculated carbonyl and carboxylic aliphatic groups (H−C−C=O)-to-total aliphatics (H−C−C=O/ΣAliphatics) and oxygenated aliphatic groups (H−C−O)-to-total aliphatics (H−C−O/ΣAliphatics), Decesari et al. (2007) created source boundaries for marine OA (MOA), SOA, and aged biomass burning OA (BBOA). Based on the source signature plot in Fig. 5, none of the WSOC samples fell into the three specific fingerprint sources previously established by Decesari et al. (2007), especially in the contribution of the H−C−C=O group. This outcome suggests that the studied WSOC samples are less oxidized than those of the predefined fingerprints, exhibiting a H−C−C=O/ΣAliphatics ratio ranging from 0.14 to 0.34, whereas the H−C−O/ΣAliphatics ratio range from 0.12 to 0.56. Interestingly, the fractional contribution of H−C−O did not vary outside of the values for the pre-established source regions, except for samples collected in Medellín, and in PV during MMB and IBB. The presence of polyols and anhydrosugars associated with pollen and fresh smoke particles (with high H−C−O/ΣAliphatics (>0.4) but low H−C−C=O/ΣAliphatics (<0.25) ratios) could contribute for the clear separation of these PM$_{10}$ samples from the remaining WSOC samples that are impacted by anthropogenic-related processes. Particularly, the aerosol WSOC samples collected in PV during IBB and MBB emissions are characterized by H−C−O/ΣAliphatics and H−C−C=O/ΣAliphatics ratios comparable to those computed for primary emissions from biomass burning (Chalbot et al., 2016) and pollen-dominated coarse particles (Chalbot et al.,
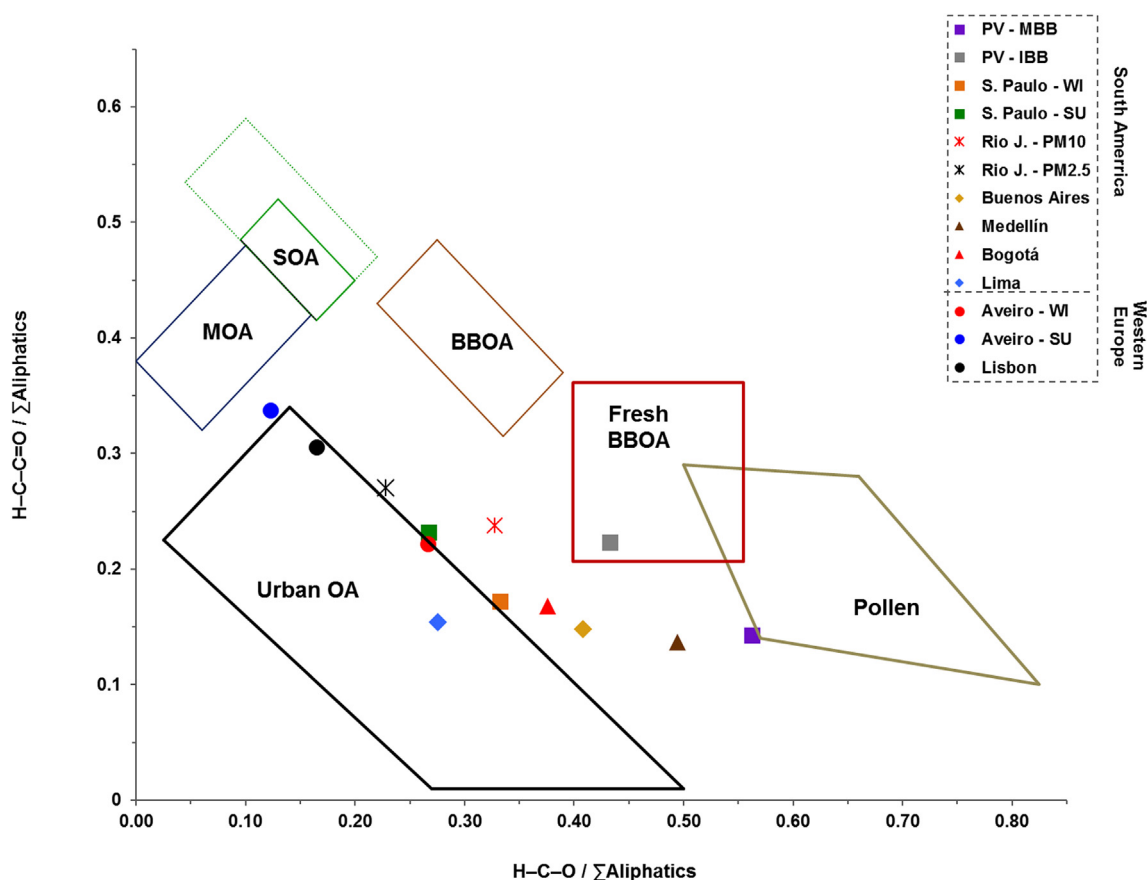
Fig. 5. Functional group distributions for WSOC from the aerosol samples collected at the different South America and Western European sites. Boxes represent boundaries for marine OA (MOA), SOA, and biomass burning OA (BBOA) based on Decesari et al. (2007), aged urban organic aerosol (Urban OA) obtained from Cleveland et al. (2012), fresh pollen (Pollen) obtained from Chalbot et al. (2014), and fresh emissions from biomass burning (fresh BBOA) obtained from Chalbot et al. (2016). Sampling periods and samples identification are given in Tables 1 and 2, respectively.

2014), respectively. According to Chalbot et al. (2016), aged and, therefore, more oxidized biomass burning OA is likely to be more depleted in polyols and phenols structures (Graham et al., 2002; Chalbot et al., 2016). Thus, samples within the biomass burning OA region firstly set by Decesari et al. (2007) may represent aged biomass burning OA, whereas those outside may be associated with fresh pollen and smoke OA emissions (Chalbot et al., 2016). The aerosol WSOC collected in Medellin differ from all the aforementioned source regions, probably reflecting the mixed contributions of biological material as well as urban and biomass burning emissions.

The remaining WSOC samples are characterized by H–C–C=O/ΣAliphatics and H–C–O/ΣAliphatics ratio values comparable to those in urban aerosols (Cleveland et al., 2012; Lopes et al., 2015). The $PM_{2.5}$ samples collected in Aveiro, Lisbon, and Rio J. during summer seasons exhibit the highest contributions of H–C–C=O structures, thus highlighting their somewhat high oxidized character. A higher oxidation level is usually associated with SOA formation (Moretti et al., 2008). However, in the context of the urban areas studied in this work, the contribution of SOA to summer WSOC samples might be covering aged primary OA emitted from non-specified anthropogenic sources (Lopes et al., 2015), either traffic or non-traffic-related fossil combustion sources. Noteworthy, the winter WSOC samples collected in Aveiro and S. Paulo exhibit lower H–C–C=O/ΣAliphatics and higher H–C–O/ΣAliphatics ratio values than the summer samples collected at the same sites, which may be explained by a higher contribution of fresh emissions, namely of smoke particles, to the winter WSOC samples.

4. Conclusions

The structural composition and ^{1}H NMR source apportionment of particulate WSOC has been described for the first time to our knowledge at different locations in South America (Medellín, Bogotá, Lima, Buenos Aires, PV in Amazon Basin, S. Paulo, and Rio J.), and further compared to those of two urban sites at the Western European coast (Aveiro and Lisbon). This study showed that the contribution of WSOC to PM mass is higher in Aveiro, Lisbon, and Rio J. than in the remaining South America locations, which points to a more oxidized character of WSOC at former urban sites, as well as differences in the aging processes and/or regional sources between South America and Western European locations.

The ^{1}H NMR data analysis also showed that all aerosol WSOC samples hold similar proton functional groups; however, they differ in terms of their relative distribution, depending on the location and time period. For most of the South American sites as well as for both Western European cities, the relative contribution of the four proton functional groups vary in the following order: H-C > H–C–C= > H-C-O > Ar-H. However, for aerosol WSOC collected in PV during MBB, Medellín, Bogotá, and Buenos Aires, the relative contribution of H-C-O structures is higher than that of H-C-C= groups. The possible key structural units of WSOC were also suggested by the ^{1}H NMR spectra. The entire region of saturated and functionalized aliphatics (most likely aliphatic carboxylic acids), which were major structural contributors to most WSOC samples, maintained its core integrity with limited, yet recognizable, variability across all samples. The most noteworthy differences

between the WSOC samples were found by far more abundant within the NMR regions assigned to carbohydrate-like and aromatic moieties. Primary saccharides, polyols, and anhydrosugars of diverse origin (e.g., fungal spores, pollen, degradation of plant material, and biomass burning), depending on the season and location, may contribute largely to the carbohydrate-related substructures. Aromatic structures with diverse substitution (e.g., -OR, -COOH, -OCH$_3$, and alkyl groups) are plausible candidates in aerosol WSOC, most of which were attributed to emissions from wood combustion, particularly during winter seasons and biomass burning events. Nevertheless, aromatic SOA might also contribute to all WSOC samples, probably related to the oxidation of aromatic hydrocarbons from urban traffic emissions.

Based on ^{1}H NMR source signatures, summer aerosol WSOC in the cities of Aveiro, Lisbon, and Rio J. has an important contribution from SOA, which are most likely associated with atmospheric aging of primary OA emitted from non-specified anthropogenic sources. Particulate WSOC in Aveiro and S. Paulo during winter are impacted by fresh emissions, namely of smoke particles, being less oxidized than those collected during the summer period. Nevertheless, the contribution of aged primary OA to these WSOC samples cannot be ruled out. Fresh primary emissions from biomass burning are undeniably the dominant source of aerosol WSOC during IBB events at the Amazon Basin. With the decline of biomass burning activities in this location, the ^{1}H NMR profile indicated the possible dominant contribution of biological particles (e.g., pollen and fungal spores) to coarse particulate WSOC. The ^{1}H NMR profiles and source attribution of particulate WSOC from Medellín, Bogotá, Buenos Aires, and Lima confirmed the mixed contributions of biological material, secondary formation, as well as urban and biomass burning emissions. In Medellín, there is a distinct contribution from biomass burning as well as biological material likely from decomposing plants or resuspension of soil dust. The particulate WSOC in Bogotá and Buenos Aires is clearly influenced by local traffic-related sources, secondary formation, and episodes of pollen release during the spring blossom.

The significant structural findings and source signatures reported in this study for aerosol WSOC in contrasting environments of South America and Western Europe, are an important diagnostic tool for understanding the role of human activities on the atmospheric load and composition of particulate organic matter at a wide geographic scale and under different environmental conditions. This study also indicates that biosphere is a major source for primary air particles at the regional scale, influencing the composition, and plausibly the atmospheric behavior, of water-soluble OA, particularly in South America.

Acknowledgments

Appendix A. Supplementary data

Supplementary data related to this article can be found at http://dx.doi.org/10.1016/j.envpol.2017.05.011.

References

Agudelo-Castañeda, D.M., Teixeira, E.C., 2014. Seasonal changes, identification and source apportionment of PAH in PM$_{1.0}$. Atmos. Environ. 96, 186—200. http://dx.doi.org/10.1016/j.atmosenv.2014.07.030.

Atkinson, R.W., Mills, I.C., Walton, H.A., Anderson, H.R., 2015. Fine particle components and health-a systematic review and meta-analysis of epidemiological time series studies of daily mortality and hospital admissions. J. Expo. Sci. Environ. Epidemiol. 25, 208—214. http://dx.doi.org/10.1038/jes.2014.63.

Bauer, H., Claeys, M., Vermeylen, R., Schueller, E., Weinke, G., Berger, A., Puxbaum, H., 2008. Arabitol and mannitol as tracers for the quantification of airborne fungal spores. Atmos. Environ. 42, 588—593. http://dx.doi.org/10.1016/j.atmosenv.2007.10.013.

Booth, B.B.B., Dunstone, N.J., Halloran, P.R., Andrews, T., Bellouin, N., 2012. Aerosols implicated as a prime driver of twentieth-century North Atlantic climate variability. Nature 484, 228—232. http://dx.doi.org/10.1038/nature10946.

Burshtein, N., Lang-Yona, N., Rudich, Y., 2011. Ergosterol, arabitol and mannitol as tracers for biogenic aerosols in the eastern Mediterranean. Atmos. Chem. Phys. 11, 829—839. http://dx.doi.org/10.5194/acp-11-829-2011.

Cassee, F.R., Héroux, M.-E., Gerlofs-Nijland, M.E., Kelly, F.J., 2013. Particulate matter beyond mass: recent health evidence on role of fractions, chemical constituents and sources of emission. Inhal. Toxicol. 25 (14), 802—812. http://dx.doi.org/10.3109/08958378.2013.850127.

Chalbot, M.-C.G., Brown, J., Chitranshi, P., Gamboa da Costa, G., Pollock, E.D., Kavouras, I.G., 2014. Functional characterization of the water-soluble organic carbon of size-fractionated aerosol in the southern Mississippi Valley. Atmos. Chem. Phys. 14, 6075—6088. http://dx.doi.org/10.5194/acp-14-6075-2014.

Chalbot, M.-C.G., Chitranshi, P., Gamboa da Costa, G., Pollock, E.D., Kavouras, I.G., 2016. Characterization of water-soluble organic matter in urban aerosol by ^{1}H-NMR spectroscopy. Atmos. Environ. 128, 235—245. http://dx.doi.org/10.1016/j.atmosenv.2015.12.067.

Cleveland, M.J., Ziemba, L.D., Griffin, R.J., Dibb, J.E., Anderson, C.H., Lefer, B., Rappengluck, B., 2012. Characterization of urban aerosol using aerosol mass spectrometry and proton nuclear magnetic resonance spectroscopy. Atmos. Environ. 54, 511—518. http://dx.doi.org/10.1016/j.atmosenv.2012.02.074.

Crilley, L.R., Ayoko, G.A., Morawska, L., 2014. First measurements of source apportionment of organic aerosols in the Southern hemisphere. Environ. Pollut. 184, 81—88. http://dx.doi.org/10.1016/j.envpol.2013.08.015.

De Oliveira Alves, N., Brito, J., Caumo, S., Arana, A., Hacon, S.S., Artaxo, P., Hillamo, R., Teinilä, K., Medeiros, S.R.B., Vasconcellos, P.C., 2015. Biomass burning in the Amazon region: aerosol source apportionment and associated health risk assessment. Atmos. Environ. 120, 277—285. http://dx.doi.org/10.1016/j.atmosenv.2015.08.059.

Decesari, S., Facchini, M.C., Fuzzi, S., McFiggans, G.B., Coe, H., Bower, K.N., 2005. The water-soluble organic component of size-segregated aerosol, cloud water and wet depositions from Jeju Island during ACE-Asia. Atmos. Environ. 39, 211—222. http://dx.doi.org/10.1016/j.atmosenv.2004.09.049.

Decesari, S., Mircea, M., Cavalli, F., Fuzzi, S., Moretti, F., Tagliavini, E., Facchini, M.C., 2007. Source attribution of water-soluble organic aerosol by nuclear magnetic resonance spectroscopy. Environ. Sci. Technol. 41, 2479—2484. http://dx.doi.org/10.1021/es061711l.

Dinar, E., Riziq, A.A., Spindler, C., Erlick, C., Kiss, G., Rudich, Y., 2008. The complex refractive index of atmospheric and model humic-like substances (HULIS) retrieved by a cavity ring down aerosol spectrometer (CRD-AS). Faraday Discuss. 137, 279—295.

Dinar, E., Taraniuk, I., Graber, E.R., Katsman, S., Moise, T., Anttila, T., Mentel, T.F., Rudich, Y., 2006. Cloud condensation nuclei properties of model and atmospheric HULIS. Atmos. Chem. Phys. 6, 2465—2482. http://dx.doi.org/10.5194/acp-6-2465-2006.

Draxler, R.R., Rolph, G.D., 2014. HYSPLIT (HYbrid Single-particle Lagrangian Integrated Trajectory) Model Access via NOAA ARL READY Website. NOAA Air Resources Laboratory, Silver Spring, MD. http://ready.arl.noaa.gov/HYSPLIT.php.

Duarte, R.M.B.O., Duarte, A.C., 2005. Application of non-ionic solid sorbents (XAD resins) for the isolation and fractionation of water-soluble organic compounds from atmospheric aerosols. J. Atmos. Chem. 51, 79—93. http://dx.doi.org/10.1007/s10874-005-8091-x.

Duarte, R.M.B.O., Freire, S.M.S.C., Duarte, A.C., 2015. Investigating the water-soluble organic functionality of urban aerosols using two-dimensional correlation of

solid-state ^{13}C NMR and FTIR spectral data. Atmos. Environ. 116, 245–252. http://dx.doi.org/10.1016/j.atmosenv.2015.06.043.

Duarte, R.M.B.O., Santos, E.B.H., Pio, C.A., Duarte, A.C., 2007. Comparison of structural features of water-soluble organic matter from atmospheric aerosols with those of aquatic humic substances. Atmos. Environ. 41, 8100–8113. http://dx.doi.org/10.1016/j.atmosenv.2007.06.034.

Duarte, R.M.B.O., Silva, A.M.S., Duarte, A.C., 2008. Two-dimensional NMR studies of water-soluble organic matter in atmospheric aerosols. Environ. Sci. Technol. 42, 8224–8230. http://dx.doi.org/10.1021/es801298s.

Elbert, W., Taylor, P.E., Andreae, M.O., Pöschl, U., 2007. Contribution of fungi to primary biogenic aerosols in the atmosphere: wet and dry discharged spores, carbohydrates, and inorganic ions. Atmos. Chem. Phys. 7, 4569–4588. http://dx.doi.org/10.5194/acp-7-4569-2007.

Fan, X., Song, J., Peng, P., 2013. Comparative study for separation of atmospheric humic-like substance (HULIS) by ENVI-18, HLB, XAD-8 and DEAE sorbents: elemental composition, FT-IR, ^{1}H NMR and off-line thermochemolysis with tetramethylammonium hydroxide (TMAH). Chemosphere 93, 1710–1719. http://dx.doi.org/10.1016/j.chemosphere.2013.05.045.

Fu, P.Q., Kawamura, K., Pavuluri, C.M., Swaminathan, T., Chen, J., 2010. Molecular characterization of urban organic aerosol in tropical India: contributions of primary emissions and secondary photooxidation. Atmos. Chem. Phys. 10, 2663–2689. http://dx.doi.org/10.5194/acp-10-2663-2010.

Fuzzi, S., Decesari, S., Facchini, M.C., Cavalli, F., Emblico, L., Mircea, M., Andreae, M.O., Trebs, I., Hoffer, A., Guyon, P., Artaxo, P., Rizzo, L.V., Lara, L.L., Pauliquevis, T., Maenhaut, W., Raes, N., Chi, X., Mayol-Bracero, O.L., Soto-García, L.L., Claeys, M., Kourtchev, I., Rissler, J., Swietlicki, E., Tagliavini, E., Schkolnik, G., Falkovich, A.H., Rudich, Y., Fisch, G., Gatti, L.V., 2007. Overview of the inorganic and organic composition of size-segregated aerosol in Rondônia, Brazil, from the biomass-burning period to the onset of wet season. J. Geophys. Res. 112, D01201. http://dx.doi.org/10.1029/2005JD006741.

Graham, B., Mayol-Bracero, O.L., Guyon, P., Roberts, G.C., Decesari, S., Facchini, M.C., Artaxo, P., Maenhaut, W., Köll, P., Andreae, M.O., 2002. Water-soluble organic compounds in biomass burning aerosols over Amazonia. 1. Characterization by NMR and GC-MS. J. Geophys. Res. 107 (NO. D20), 8047. http://dx.doi.org/10.1029/2001JD000336.

Hallquist, M., Wenger, J.C., Baltensperger, U., Rudich, Y., Simpson, D., Claeys, M., Dommen, J., Donahue, N.M., George, C., Goldstein, A.H., Hamilton, J.F., Herrmann, H., Hoffmann, T., Iinuma, Y., Jang, M., Jenkin, M.E., Jimenez, J.L., Kiendler-Scharr, A., Maenhaut, W., McFiggans, G., Mentel, ThF., Monod, A., Prévôt, A.S.H., Seinfeld, J.H., Surratt, J.D., Szmigielski, R., Wildt, J., 2009. The formation, properties and impact of secondary organic aerosol: current and emerging issues. Atmos. Chem. Phys. 9, 5155–5236. http://dx.doi.org/10.5194/acp-9-5155-2009.

Heal, M.R., Kumar, P., Harrison, R.M., 2012. Particles, air quality, policy and health. Chem. Soc. Rev. 41, 6606–6630. http://dx.doi.org/10.1039/c2cs35076a.

Iinuma, Y., Böge, O., Herrmann, H., 2010. Methyl-nitrocatechols: atmospheric tracer compounds for biomass burning secondary organic aerosols. Environ. Sci. Technol. 44, 8453–8459. http://dx.doi.org/10.1021/es102938a.

Jimenez, J.L., Canagaratna, M.R., Donahue, N.M., Prevot, A.S.H., Zhang, Q., Kroll, J.H., DeCarlo, P.F., Allan, J.D., Coe, H., Ng, N.L., Aiken, A.C., Docherty, K.S., Ulbrich, I.M., Grieshop, A.P., Robinson, A.L., Duplissy, J., Smith, J.D., Wilson, K.R., Lanz, V.A., Hueglin, C., Sun, Y.L., Tian, J., Laaksonen, A., Raatikainen, T., Rautiainen, J., Vaattovaara, P., ehn, M., Kulmala, M., Tomlinson, J., Collins, D.R., Cubison, M.J., Dunlea, E.J., Huffman, A., Onasch, T.B., Alfarra, M.R., Williams, P.I., Bower, K.N., Kondo, Y., Schneider, J., Drewnick, F., Borrmann, S., Weimer, S., Demerjian, K.L., Salcedo, D., Cottrell, L., Griffin, R., Takami, A., Miyoshi, T., Hatakeyama, S., Jayne, J.T., Herndon, S.C., Trimborn, A., Williams, L.R., Wood, E.C., Middlebrook, A., Kolb, C.E., Baltensperger, U., Worsnop, D.R., 2009. Evolution of organic aerosols in the atmosphere. Science 326, 1525–1529. http://dx.doi.org/10.1126/science.1180353.

Jurado, E., Dachs, J., Duarte, C.M., Simó, R., 2008. Atmospheric deposition of organic and black carbon to the global oceans. Atmos. Environ. 42, 7931–7939. http://dx.doi.org/10.1016/j.atmosenv.2008.07.029.

Kanakidou, M., Seinfeld, J.H., Pandis, S.N., Barnes, I., Dentener, F.J., Facchini, M.C., Van Dingenen, R., Ervens, B., Nenes, A., Nielsen, C.J., Swietlicki, E., Putaud, J.-P., Balkanski, Y., Fuzzi, S., Horth, J., Moortgat, G.K., Winterhalter, R., Myhre, C.E.L., Tsigaridis, K., Vignati, E., Stephanou, E.G., Wilson, J., 2005. Organic aerosol and global climate modelling: a review. Atmos. Chem. Phys. 5, 1053–1123. http://dx.doi.org/10.5194/acp-5-1053-2005.

Laskin, A., Laskin, J., Nizkorodov, S.A., 2015. Chemistry of atmospheric brown carbon. Chem. Rev. 115, 4335–4382. http://dx.doi.org/10.1021/cr5006167.

Lee, H.J., Aiona, P.K., Laskin, A., Laskin, J., Nizkorodov, S.A., 2014. Effect of solar radiation on the optical properties and molecular composition of laboratory proxies of atmospheric brown carbon. Environ. Sci. Technol. 48, 10217–10226. http://dx.doi.org/10.1021/es502515r.

Liang, L., Engling, G., He, K., Du, Z., Cheng, Y., Duan, F., 2013. Evaluation of fungal spore characteristics in Beijing, China, based on molecular tracer measurements. Environ. Res. Lett. 8, 014005. http://dx.doi.org/10.1088/1748-9326/8/1/014005.

Lopes, C.B., Abreu, S., Válega, M., Duarte, R.M.B.O., Pereira, M.E., Duarte, A.C., 2006. The assembling and application of an automated segmented flow analyzer for the determination of dissolved organic carbon based on UV-persulphate oxidation. Anal. Lett. 39, 1979–1992. http://dx.doi.org/10.1080/00032710600723908.

Lopes, S.P., Matos, J.T.V., Silva, A.M.S., Duarte, A.C., Duarte, R.M.B.O., 2015. ^{1}H NMR

studies of water- and alkaline-soluble organic matter from fine urban atmospheric aerosols. Atmos. Environ. 119, 374–380. http://dx.doi.org/10.1016/j.atmosenv.2015.08.072.

Mayol-Bracero, O.L., Guyon, P., Graham, B., Roberts, G., Andreae, M.O., Decesari, S., Facchini, M.C., Fuzzi, S., Artaxo, P., 2002. Water-soluble organic compounds in biomass burning aerosols over Amazonia. 2. Apportionment of the chemical composition and importance of the polyacidic fraction. J. Geophys. Res. 107 (NO. D20), 8091. http://dx.doi.org/10.1029/2001JD000522.

Minguillón, M.C., Pérez, N., Marchand, N., Bertrand, A., Temime-Roussel, B., Agrios, K., Szidat, S., van Drooge, B., Sylvestre, A., Alastuey, A., Reche, C., Ripoll, A., Marco, E., Grimalt, J.O., Querol, X., 2016. Secondary organic aerosol origin in an urban environment: influence of biogenic and fuel combustion precursors. Faraday Discuss. 189, 337–359. http://dx.doi.org/10.1039/c5fd00182j.

Mkoma, S.L., Kawamura, K., 2013. Molecular composition of dicarboxylic acids, ketocarboxylic acids, α-dicarbonyls and fatty acids in atmospheric aerosols from Tanzania, East Africa during wet and dry seasons. Atmos. Chem. Phys. 13, 2235–2251. http://dx.doi.org/10.5194/acp-13-10325-2013.

Mladenov, N., Reche, I., Olmo, F.J., Lyamani, H., Alados-Arboledas, L., 2010. Relationships between spectroscopic properties of high-altitude organic aerosols and sun photometry from ground-based remote sensing. J. Geophys. Res. 115, G00F11. http://dx.doi.org/10.1029/2009JG000991.

Moretti, F., Tagliavini, E., Decesari, S., Facchini, M.C., Rinaldi, M., Fuzzi, S., 2008. NMR determination of total carbonyls and carboxyls: a tool for tracing the evolution of atmospheric oxidized organic aerosols. Environ. Sci. Technol. 42, 4844–4849. http://dx.doi.org/10.1021/es703166v.

Ng, N.L., Canagaratna, M.R., Zhang, Q., Jimenez, J.L., Tian, J., Ulbrich, I.M., Kroll, J.H., Docherty, K.S., Chhabra, P.S., Bahreini, R., Murphy, S.M., Seinfeld, J.H., Hildebrandt, L., Donahue, N.M., DeCarlo, P.F., Lanz, V.A., Prévôt, A.S.H., Dinar, E., Rudich, Y., Worsnop, D.R., 2010. Organic aerosol components observed in Northern Hemispheric datasets from aerosol mass spectrometry. Atmos. Chem. Phys. 10, 4625–4641. http://dx.doi.org/10.5194/acp-10-4625-2010.

Padró, L.T., Tkacik, D., Lathem, T., Hennigan, C.J., Sullivan, A.P., Weber, R.J., Huey, L.G., Nenes, A., 2010. Investigation of cloud condensation nuclei properties and droplet growth kinetics of the water-soluble aerosol fraction in Mexico City. J. Geophys. Res. 115, D09204. http://dx.doi.org/10.1029/2009JD013195.

Paglione, M., Saarikoski, S., Carbone, S., Hillamo, R., Facchini, M.C., Finessi, E., Giulianelli, L., Carbone, C., Fuzzi, S., Moretti, F., Tagliavini, E., Swietlicki, E., Stenström, K.E., Prévôt, A.S.H., Massoli, P., Canaragatna, M., Worsnop, D., Decesari, S., 2014. Primary and secondary biomass burning aerosols determined by proton nuclear magnetic resonance (1H-NMR) spectroscopy during the 2008 EUCAARI campaign in the Po Valley (Italy). Atmos. Chem. Phys. 14, 5089–5110. http://dx.doi.org/10.5194/acp-14-5089-2014.

Pietrogrande, M.C., Bacco, D., Chiereghin, S., 2013. GC/MS analysis of water-soluble organics in atmospheric aerosol: optimization of a solvent extraction procedure for simultaneous analysis of carboxylic acids and sugars. Anal. Bioanal. Chem. 405, 1095–1104. http://dx.doi.org/10.1007/s00216-012-6592-4.

Putaud, J.-P., Van Dingenen, R., Alastuey, A., Bauer, H., Birmili, W., Cyrys, J., Flentje, H., Fuzzi, S., Gehrig, R., Hansson, H.C., Harrison, R.M., Herrmann, H., Hitzenberger, R., Hüglin, C., Jones, A.M., Kasper-Giebl, A., Kiss, G., Kousam, A., Kuhlbusch, T.A.J., Löschau, G., Maenhaut, W., Molnar, A., Moreno, T., Pekkanen, J., Perrino, C., Pitz, M., Puxbaum, H., Querol, X., Rodriguez, S., Salma, I., Schwarz, J., Smolik, J., Schneider, J., Spindler, G., ten Brink, H., Tursic, J., Viana, M., Wiedensohler, A., Raes, F., 2010. A European aerosol phenomenology – 3: physical and chemical characteristics of particulate matter from 60 rural, urban, and kerbside sites across Europe. Atmos. Environ 44, 1308–1320. http://dx.doi.org/10.1016/j.atmosenv.2009.12.011.

Rolph, G.D., 2014. Real-time Environmental Applications and Display SYstem (READY) Website. NOAA Air Resources Laboratory, Silver Spring, MD. http://ready.arl.noaa.gov.

Saffari, A., Daher, N., Shafer, M.M., Schauer, J.J., Sioutas, C., 2014. Global perspective on the oxidative potential of airborne particulate matter: a synthesis of research findings. Environ. Sci. Technol. 48, 7576–7583. http://dx.doi.org/10.1021/es500937x.

Shakya, K.M., Place Jr., P.F., Griffin, R.J., Talbot, R.W., 2012. Carbonaceous content and water-soluble organic functionality of atmospheric aerosols at a semi-rural New England location. J. Geophys. Res. 117, D03301. http://dx.doi.org/10.1029/2011JD016113.

Song, J., He, L., Peng, P., Zhao, J., Ma, S., 2012. Chemical and isotopic composition of humic-like substances (HULIS) in ambient aerosols in Guangzhou, South China. Aerosol Sci. Technol. 46 (5), 533–546. http://dx.doi.org/10.1080/02786826.2011.645956.

Souza, D.Z., Vasconcellos, P.C., Lee, H., Aurela, M., Saarnio, K., Teinilä, K., Hillamo, R., 2014. Composition of PM$_{2.5}$ and PM$_{10}$ collected at urban sites in Brazil. Aerosol Air Qual. Res. 14, 168–176. http://dx.doi.org/10.4209/aaqr.2013.03.0071.

Tagliavini, E., Moretti, F., Decesari, S., Facchini, M.C., Fuzzi, S., Maenhaut, W., 2006. Functional group analysis by H NMR/chemical derivatization for the characterization of organic aerosol from the SMOCC field campaign. Atmos. Chem. Phys. 6, 1003–1019. http://dx.doi.org/10.5194/acp-6-1003-2006.

Timonen, H., Carbone, S., Aurela, M., Saarnio, K., Saarikoski, S., Ng, N.L., Canagaratna, M.R., Kulmala, M., Kerminen, V.-M., Worsnop, D.R., Hillamo, R., 2013. Characteristics, sources and water-solubility of ambient submicron organic aerosol in springtime in Helsinki, Finland. J. Aerosol Sci. 56, 61–77. http://dx.doi.org/10.1016/j.jaerosci.2012.06.005.

Vargas, F.A., Rojas, N.Y., Pachon, J.E., Russell, A.G., 2012. PM$_{10}$ characterization and

source apportionment at two residential areas in Bogota. Atmos. Poll. Res. 3 (1), 72—80. http://dx.doi.org/10.5094/APR.2012.006.

Vasconcellos, P.C., Souza, D.Z., Ávila, S.G., Araújo, M.P., Naoto, E., Nascimento, K.H., Cavalcante, F.S., Santos, M., Patricia Smichowski, P., Behrentz, E., 2011. Comparative study of the atmospheric chemical composition of three South American cities. Atmos. Environ. 45, 5770—5777. http://dx.doi.org/10.1016/j.atmosenv.2011.07.018.

Vasconcellos, P.C., Souza, D.Z., Ccoyllo, O., Bustillos, J.O., Lee, H., Santos, F.C., Nascimento, K.H., Araújo, M.P., Saarnio, K., Teinila, K., Hillamo, R., 2010. Determination of anthropogenic and biogenic compounds on atmospheric aerosol collected in urban, biomass burning and forest areas in São Paulo. Braz. Sci. Total Environ. 408, 5836—5844. http://dx.doi.org/10.1016/j.scitotenv.2010.08.012.

Villalobos, A.M., Barraza, F., Jorquera, H., Schauer, J.J., 2015. Chemical speciation and source apportionment of fine particulate matter in Santiago, Chile, 2013. Sci. Total Environ. 512—513, 133—142. http://dx.doi.org/10.1016/j.scitotenv.2015.01.006.

Wozniak, A.S., Bauer, J.E., Dickhut, R.M., 2012. Characteristics of water-soluble organic carbon associated with aerosol particles in the eastern United States. Atmos. Environ. 46, 181—188. http://dx.doi.org/10.1016/j.atmosenv.2011.10.001.

Zhang, Q., Jimenez, J.L., Canagaratna, M.R., Allan, J.D., Coe, H., Ulbrich, I., Alfarra, M.R., Takami, A., Middlebrook, A.M., Sun, Y.L., Dzepina, K., Dunlea, E., Docherty, K., DeCarlo, P.F., Salcedo, D., Onasch, T., Jayne, J.T., Miyoshi, T., Shimono, A., Hatakeyama, S., Takegawa, N., Kondo, Y., Schneider, J., Drewnick, F., Borrmann, S., Weimer, S., Demerjian, K., Williams, P., Bower, K., Bahreini, R., Cottrell, L., Griffin, R.J., Rautiainen, J., Sun, J.Y., Zhang, Y.M., Worsnop, D.R., 2007. Ubiquity and dominance of oxygenated species in organic aerosols in anthropogenically-influenced Northern Hemisphere midlatitudes. Geophys. Res. Lett. 34, L13801. http://dx.doi.org/10.1029/2007GL029979.

Zhang, Y., Liu, J., Salazar, G.A., Li, J., Zotter, P., Zhang, G., Shen, R., Schäfer, K., Schnelle-Kreis, J., Prèvôt, A.S.H., Szidat, S., 2014. Micro-scale (μg) radiocarbon analysis of water-soluble organic carbon in aerosol samples. Atmos. Environ. 97, 1—5. http://dx.doi.org/10.1016/j.atmosenv.2014.07.059.